

Axial Magnetic Field Measurements of Pulsed Solenoids

J. Novickij, R. Kačianauskas, A. Kačeniauskas

Vilnius Gediminas Technical University, Saulėtekio al.11, LT-10223, Vilnius, Lithuania; e-mail:elektrotechnika@el.vtu.lt

S. Balevičius, N. Žurauskienė, V. Stankevič

Semiconductor Physics Institute, A. Goštauto 11, LT-01108, Vilnius, Lithuania; e-mail:sbal@pfi.lt

Introduction

Magnetic field is a powerful instrument for scientific researches and industrial applications. Important discoveries were done whenever the magnetic field generated by laboratory magnets was increased. It is very important to improve the laboratory facilities in order to achieve the value of magnetic field as much as possible. But the increase of magnetic field is accompanied by quadratic increase of electrical, thermal and mechanical loads. Therefore, high magnetic field generation is not a trivial aim and it requires a lot of attempts solving technical problems.

Traditionally there are two main techniques to generate magnetic fields: static and pulsed magnetic field generation. Historically magnetic field generation technique was started from Oersted and Ampere investigation of electromagnets. A classical construction of permanent electromagnets successfully was used during almost two hundred years without principal changes. The permanent electromagnet with iron core became an ordinary facility at universities and research centers. The highest DC fields of 45 T are obtained in a "hybrid magnet" designed at the National High Magnetic Field Laboratory (NHMFL), USA. Investigations using steady magnetic fields up to 20-40T require a power energy source of 25-50MW as minimum. The expensive DC high magnetic field facilities can be replaced in many experiments by the application of pulsed field technique, pioneered by P. Kapitza. The technique is based on storing the energy in different kinds of storage as capacitor bank, inductivity, kinetic energy of a rotor, explosives and the following discharging the energy bank through a pulsed inductor during a short period of time. The reduction of the time scale has an amplifying effect upon the magnetic field. Therefore, pulsed magnetic fields of 20-40T became attractive in most experiments for investigations at high magnetic fields [2]. The most recent efforts of scientists were directed to the development of a non-destructive pulsed magnetic field up to 100 T. Pulsed very high magnetic field facilities are also expensive and unique as DC magnets, and, therefore, are concentrated in famous universities and laboratories as NHMFL, Leuven,

Amsterdam, Oxford, Toulouse, Berlin, Grenoble Universities and other centers [1].

It is necessary to separate pulsed magnetic fields into two categories: non-destructively and destructively generated magnetic fields.

The destruction of the conductor material by Joule heating and mechanical deformation determines the highest field that can be obtained with laboratory device. The dominant factor in magnet design is mechanical strength of the construction which has to withstand large magnetic forces. This becomes quite critical in magnetic fields more than 25-35T, when magnetic forces exceed the mechanical strength of a cooper. Pulsed coils should be reinforced with a steel or other mechanically strong material cylinder to avoid the destruction of the coil due to shock waves. The application of traditional cooper wires is limited by magnetic induction up to 35-40T, beryllium-cooper up to 50-60T, Nb-Cu alloys up to 60-70T. Recently the interest to generate non-destructive fields up to 100T increased very much [3]. Famous laboratories in Oxford, Leuven, Toulouse and others have put great efforts to achieve non-destructive pulsed magnetic fields in megagauss area [4]. During destructive or one shot experiments, a maximal magnetic field can reach the value from hundred up to few thousand Tesla (maximal magnetic field of 2800T was obtained by explosive flux compression method in Sarov, Russia). In these experiments the general aim is the generation of the magnetic field as high as possible. The magnetic field homogeneity is a secondary factor [5].

Vilnius High Magnetic Field Centre created as joint scientific research activities of Semiconductor Physics Institute and Vilnius Gediminas Technical University has developed a compact pulsed high magnetic field generator. Magnetic fields with the maximum amplitude of 48T and duration of 0.1-2 ms are generated using reinforced solenoids. The solenoid geometry is optimized to insure acceptable measurement accuracy.

Magnetic field of pulsed solenoids

Non-destructive multilayer solenoids are commonly used in material science measurements. A cross-section of such construction is schematically shown in Fig. 1.

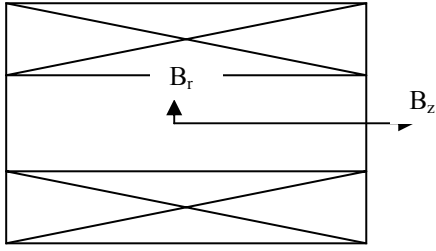


Fig. 1. Solenoid cross-section

Generated magnetic field B in central area can be calculated by the formula [6]

$$B = \mu_0 \frac{NI}{r_1} \left[\frac{F(\alpha, \beta)}{2\beta(\alpha - 1)} \right], \quad (1)$$

where μ_0 is the magnetic constant, N is the quantity of turns, I is the current, r_1 , r_2 , l are internal, external radius and length of the solenoid respectively, $\alpha = \frac{r_2}{r_1}$, $\beta = \frac{l}{2r_1}$ are relative sizes and

$F(\alpha, \beta) = \beta \ln \frac{\alpha + \sqrt{\alpha^2 + \beta^2}}{1 + \sqrt{1 + \beta^2}}$ is a form factor of the solenoid.

Magnetic induction in any point of the coil can be expressed as

$$B_z(\rho, \theta) = B \left[1 + E_2 \left(\frac{\rho}{r_1} \right)^2 P_2(u) + E_4 \left(\frac{\rho}{r_1} \right)^4 P_4(u) + \dots \right],$$

$$B_r(\rho, \theta) = B \left[0 + E_2 \left(\frac{\rho}{r_1} \right)^2 P_2'(u) + E_4 \left(\frac{\rho}{r_1} \right)^4 P_4'(u) + \dots \right]. \quad (2)$$

where, $B_z(\rho, \theta)$, $B_r(\rho, \theta)$ are axial and radial components of magnetic field in the point with spherical coordinates r, θ , and $P_n(u)$, $P_n'(u)$ are Legendre polynomial and its derivative, respectively. $u = \cos \theta$, E_n are coefficients for partial field derivative in point $z = 0$ determined by Taylor's formula

$$E_{2n} = \frac{1}{H_0} \frac{1}{(2n)!} \frac{\partial^{2n} H_z(z, 0)}{\partial z^{2n}} \Big|_{z=0}. \quad (3)$$

The axial and radial non-homogeneity of the magnetic field in the central area of the solenoid are shown in Fig. 2 and Fig. 3, respectively. It is possible to determine the maximal area inside a solenoid where magnetic field distortions do not exceed the acceptable value. The above mentioned method provides a preliminary estimation of the field non-homogeneity and does not include the influence of mechanical stresses, technological factors as a layer filling factor, reinforcement and others. But in any case the preliminary estimation is necessary to avoid further measurement mistakes. Using the special software it is possible to introduce addition factors and to simulate the discharge of a capacitor bank through the solenoid with real parameters [7].

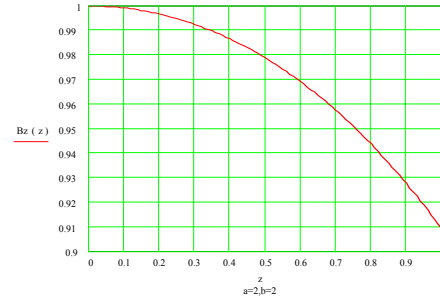


Fig. 2. Axial magnetic field $B_z(z)$, $z = z/r_1$

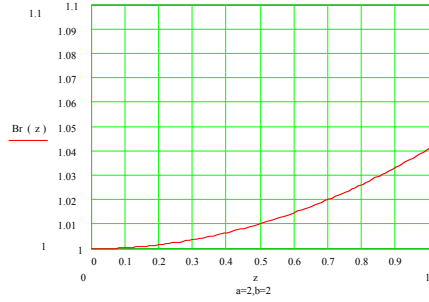


Fig. 3. Radial magnetic field $B_r(z)$, $z = z/r_1$

The radial non-homogeneity of pulsed magnetic field is two times less than the axial one and the determination of the non-homogeneity of generated magnetic field inside the pulsed magnet can be reduced only to the estimation of axial non-homogeneity.

The design of the solenoid involves many degrees of freedom. In most applications the inner coil radius, pulse duration, peak magnetic field, and non-homogeneity of magnetic field are the basic parameters for further calculations. The final form of the solenoid is defined by a lot of parameters and steps of the optimization. An analytical calculation could be performed only after carefully reduced problem to most significant parameters. In this way the model becomes useful for the analytical calculation. Recently the computing power is increased very much and such numerical methods as finite elements, finite differences are used for pulsed magnet design calculations. The most complex solenoid geometry with real physical parameters can be calculated under the acceptable precision. Sometimes the more factors you put into mathematical model the less practical interest of numerical simulations will take place. Therefore, numerically obtained results always have to be compared with the experimental data. For example, the optimization steps of coil geometry to find a maximal available magnetic field not taking into account mechanical stress analysis have no practical interest in high magnetic field area. In the first step thermal and mechanical stresses should be carefully estimated. As to axial magnetic field analysis it is limited by basic analytic formulas in the most cases.

Axial magnetic field measurements

Analytic and numerical simulation of generated magnetic field helps to verify many constructing ideas. However, in any case the validity of calculations should be

compared with experimental results. Fig. 4 presents the photo of fabricated solenoid.

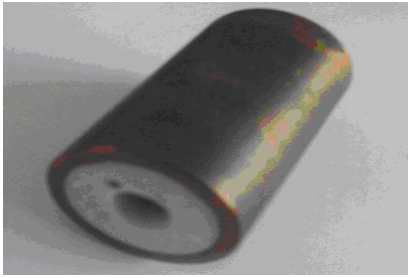


Fig. 4. Pulsed solenoid

The solenoid was fabricated using multilayer technology and included 6 layers of cooper wire wounded in 19 turns in each layer. Every layer was insulated with epoxy impregnated glass fibre. The inside diameter of the solenoid is 12 mm, the outside diameter is 32 mm, and the length is 30 mm. The solenoid was mounted into a special steel container as shown in Fig. 5.

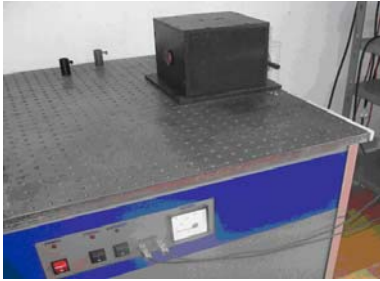


Fig. 5. Steel container

The pulsed power generator consists of 5000μF capacitor bank, the high power thyristor switch, the special steel container, and recoding system. The steel container is used for security purposes. The operation voltage can be adjusted from 100 to 4500V. A pulse of magnetic field up to 48 T is generated discharging a capacitor bank (total energy of 50 kJ) through the solenoid. The pulse duration is 2 ms. The generated pulse shape is shown in Fig. 6.

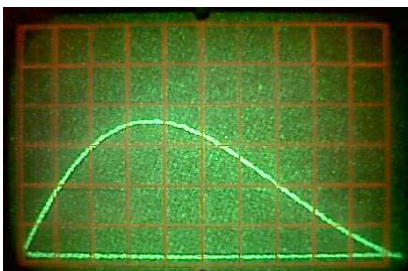


Fig. 6. Magnetic field pulse.

A magnetic field created by a stranded coil in infinite domain can be calculated analytically [9]:

$$\mathbf{H}_z = \frac{1}{2} \mathbf{J}_s \left(h_1 \ln \frac{b + \sqrt{b^2 + h_1^2}}{a + \sqrt{a^2 + h_1^2}} + h_2 \ln \frac{b + \sqrt{b^2 + h_2^2}}{a + \sqrt{a^2 + h_2^2}} \right), \quad (4)$$

here a is the internal radius of the turns region, b is the external radius of the turns region, h_1 and h_2 are local z coordinates. The axial magnetic field of the pulsed solenoid was numerically analysed using the finite element method and the software ANSYS [8]. A high magnetic field was described by Maxwell equations. The non-linear dynamic analysis of the short field pulse was performed in the axisymmetric solution domain including the complete solenoid construction. The finite element method analysis of axial magnetic field was based on the numerical model:

$$\left[C^M \right] \left\{ \dot{A} \right\} + \left[K^M(A) \right] \left\{ A \right\} = \left\{ J \right\}, \quad (5)$$

here $\{A\}$ is magnetic vector potential; $\{\dot{A}\}$ is the first time derivative of magnetic vector potential; $[K^M]$ and $[C^M]$ are coefficient matrices of Maxwell equations; $\{J\}$ is current density vector. The model was validated performing quantitative comparison of numerical results with experimental measurements and analytical solution. The quantitative comparison of the analytical solution and numerical results obtained using different boundary conditions is shown in Fig. 7.

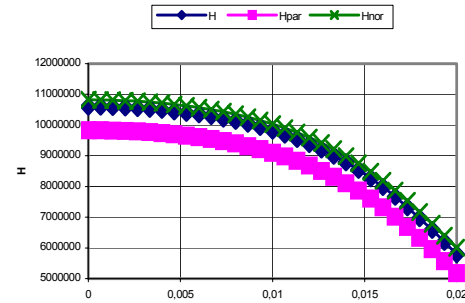


Fig. 7. The quantitative comparison of the analytical solution and numerical results

The curve H_{nor} presents distribution of magnetic field intensity along the axis z computed using Dirichlet boundary conditions. The curve H_{par} shows the numerical solution obtained employing Newman boundary conditions. The numerical error equals to about 2% and illustrates the insensitivity of the model to boundary conditions. Experimental results of axial magnetic field were measured using two methods. The first method is based on measurement of time derivative of magnetic induction from which pulsed magnetic field value could be obtained. The signal was indicated by pick-up coil located in pulsed solenoid. A pick-up coil was connected with RC-integrator circuit. Measuring scheme and photo of pick-up coil is shown in Fig. 8

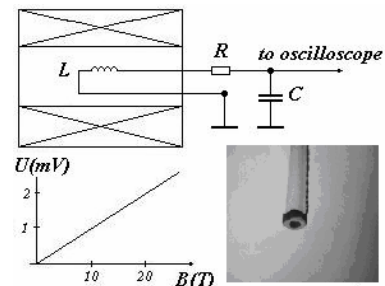


Fig. 8. Measuring scheme, output signal and a photo of pick-up coil

Output signal of the integer is equal

$$U_{out} = \frac{1}{RC} \int_0^t U_{in}(t) \exp\left(-\frac{\tau-t}{RC}\right) dt. \quad (6)$$

If the integer constant $RC \gg \tau$, where τ is the pulse duration, the integer output signal is proportional to magnetic field induction and can be expressed as

$$B = \frac{URC}{NS}, \quad (7)$$

here U is the integer output signal, RC is integer constant, N is number of turns of pick-up coil with cross-section S . Axial magnetic field distribution was measured by means of shifting pick-up coil along axial direction (Fig. 9).

The difference between experimental and calculated data is about 2-3%. This means that mathematical model of investigated pulsed solenoid is in a good agreement with experimental results. Therefore, pick-up measurements of axial magnetic field have the acceptable accuracy for the most experiments. A pick-up coil should be positioned very carefully to insure the rectangular orientation between vector of magnetic induction and the surface of the pick-up inducting coil. A neglectful inequality introduces drastic errors in measurement results. In this situation it is important to find alternative facilities to measure axial magnetic field. One of the possible ways is measurement using solid state sensors. Hall sensors are not acceptable for high magnetic field measurements because of quantum effects in semiconductors.

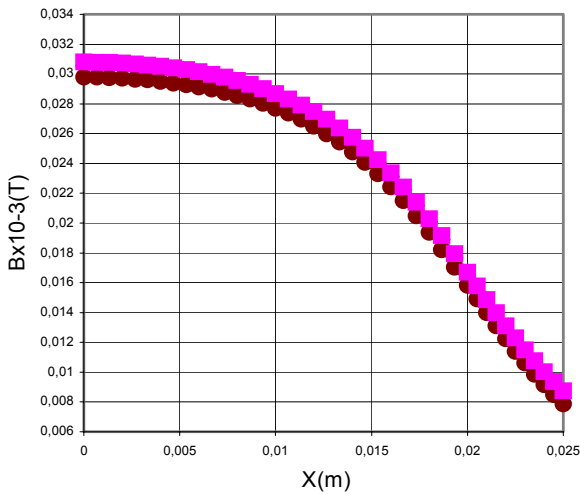
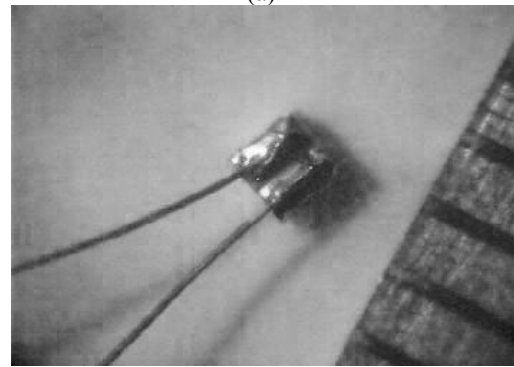
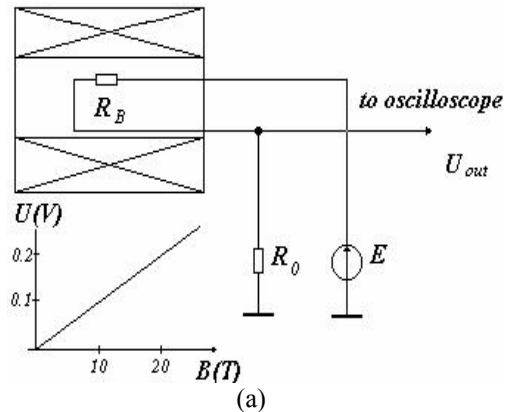


Fig.9. Axial magnetic field measurement

The phenomenon of colossal magnetoresistance in $La_{0.67}Ca_{0.33}MnO_3$ could be used for the development of high magnetic field sensors. The investigations of electrical properties of $La-Ca-Mn-O$ thin films in pulsed magnetic fields were performed at the Semiconductor Physics Institute [10]. The thin $La_{0.67}Ca_{0.33}MnO_3$ films were deposited by $Nd^{3+}YAG$ laser ablation onto MgO substrates. The thickness of the films was about 140 nanometers. The samples used for pulsed magnetic field measurements were prepared in the shape of strips having two Ag electrodes. The dimensions of the strips were $1mm$

x $1mm$, the distance between electrodes was 50 micrometers. The resistance of the sample was about 1000 Ohm at room temperature. The schematic diagram of measurements, output signal (a) and a view of the described sample (b) is shown in Fig.10.



(b)

Fig.10. The schematic diagram of measurements, output signal (a) and a $La-Ca-Mn-O$ sample (b).

A pulsed magnetic field was generated with the reinforced solenoid as was described above. The comparison of output signals of peak-up inducting coil and $La-Ca-Mn-O$ sample is shown in Fig.11.

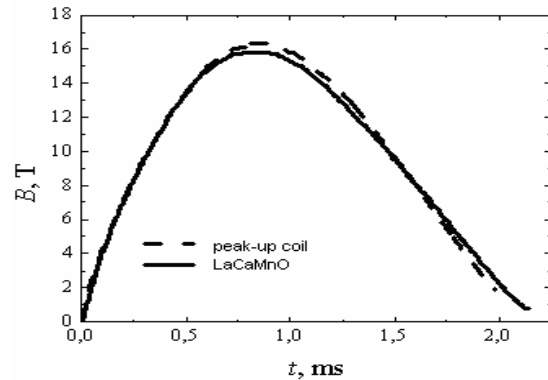


Fig.11. Magnetic field pulse registered with peak-up coil and $La-Ca-Mn-O$ sample

After further calibration of $La-Ca-Mn-O$ sample, measurements of axial magnetic field were performed. The sample was displaced with the scanning mechanism along axial direction of the pulsed solenoid after every shot. Measurements were done in 40 different points. Such measurements were also done using pick-up inducting coil. Experimental results were compared with computed axial magnetic field and are shown in Fig. 12.

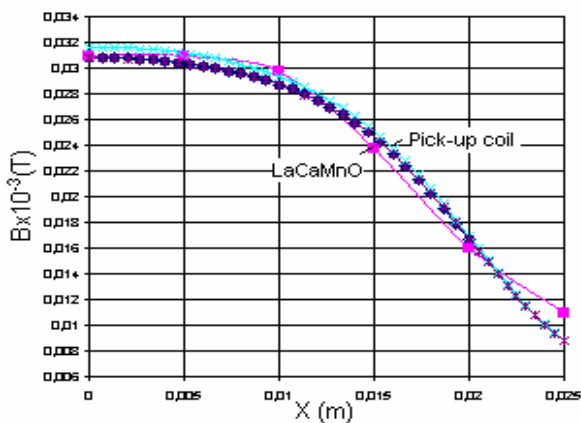


Fig. 12. Axial magnetic field measurements using *La-Ca-Mn-O* sample, pick-up coil

Obtained experimental results are in a good agreement with calculated axial magnetic field. Therefore, if the geometry of a pulsed solenoid is well known, it is not necessary to measure the field distribution. The preliminary estimation of the field distortions using analytic formulas is an adequate in the most applications (error does not exceed 3-5%). However, it is correct only for multilayer and multi-turn pulsed magnets with constant current distribution. For precise measurements experimental pulsed magnetic field calibration is required in any case.

Conclusions

The analysis of axial magnetic field of pulsed solenoids was performed. Axial magnetic field was estimated using analytical and numerical methods of magnetic field simulation. It was found that the boundary conditions can be not taken into consideration for most common applications. An analytical simulation and numerical one proposes the similar results. Calculated results of axial magnetic field were checked by measurements of axial magnetic field distribution using the

pick-up inducting coil and $La_{0.67}Ca_{0.33}MnO_3$ sample. Experimental results confirmed a good agreement of measured axial magnetic field and the computing data.

Acknowledgement

The investigations are supported by the Lithuanian Science and Studies Foundation under the contract No. K-058.

References

1. **Herlach F.** Laboratory electromagnets-from Oersted to megagauss // *Physica B.-Elsevier*, North-Holland, 2002.– Vol. 319. – P. 321-329.
2. **Herlach F.** Strong and ultrastrong magnetic fields and their applications // Springer-Verlag, Berlin, 1985. – P. 248-279.
3. **Kindo K.** 100T magnet developed in Osaka // *Physica B.-Elsevier*, North-Holland, 2001. – Vol. 294-295. – P. 585-590.
4. **Askenasy S.** A Leuven type coil in a coilex for 100T non-destructive magnets// *Physica B.-Elsevier*, North-Holland, 1998. – Vol.2 46-247. – P. 67-72.
5. **Kakol T.** The optimal coil build-up armed to generate high pulsed magnetic fields // *Physica B.-Elsevier*, North-Holland, 2001. – Vol. 298. – P. 594-598.
6. **Montgomery D.** Solenoid Magnet Design // Wiley-Interscience Division of John Wiley and Sons, NY, 1969. – P. 159.
7. **Vanacken J.** Pulsed magnet design software // *Physica B.-Elsevier*, North-Holland, 2001. – Vol. 294-295. –P. 674-678.
8. **ANSYS** Theory Reference, 8th edition, SAS IP INC, 1997.
9. **Knoepfel H.** Pulsed Magnetic Fields // North-Holland Publishing Company, Amsterdam, 1970. – P.5-40.
10. **Balevicius S., Vengalis B., Anisimovas F.** and all Relaxation of LaCaMnO films resistance in pulsed high magnetic fields // *Jornal of Low Temperature Physics*, Kluwer Academic Plenum Publishers, Belgium, 1999. – Vol.117, Nr.5/6. – P.1653-1657.

Pateikta spaudai 2004 03 02

J. Novickij, R. Kačianauskas, A. Kačeniauskas, S. Balevičius, N. Žurauskienė, V. Stankevič. Impulsinių solenoidų ašinio magnetinio lauko matavimas // *Elektronika ir elektrotechnika*. – Kaunas: Technologija, 2004.-Nr. 2(51). – P. 15-19.

Nagrinėjami impulsinio solenoido magnetinio lauko matavimai. Ašinis magnetinis laukas įvertintas taikant skaitmeninius ir analizinius metodus. Gauti rezultatai panašūs. Skaičiavimo rezultatai buvo palyginti su eksperimentiniais rezultatais, gautais matuojant ašinį magnetinį lauką indukcinė rite ir *LaCaMnO* davikliu. Matavimo rezultatai paklaidų ribose sutampa su skaičiavimo rezultatais. Il.12, bibl.10 (anglų kalba, santraukos lietuvių, anglų ir rusų k.)

J. Novickij, R. Kačianauskas, A. Kačeniauskas, S. Balevičius, N. Žurauskienė, V. Stankevič. Axial Magnetic Field Measurements of Pulsed Solenoids // *Electronics and Electrical Engineering*. – Kaunas: Technologija, 2004. – No. 2(51). – P.15-19.

Magnetic field measurement of pulsed solenoids is described. Axial magnetic field is estimated using analytical and numerical methods. Analytical simulation and numerical one proposes the approximate results. Computing results were verified by axial magnetic field measurements using pick-up inducting coil and *LaCaMnO* sample. Applied results confirmed a good coincidence of experimental values of axial magnetic field and computing data. Il. 2, bibl. 10 (in English; summaries in Lithuanian, English and Russian).

Ю. Новицкий, Р. Качанаускас, А. Каченяускас, С. Балявичюс, Н. Жураускаене, В. Станкевич. Измерение аксиального магнитного поля импульсного соленоида // *Электроника и электротехника*. – Каунас.Технология, 2004. – № 2(51). – С.15-19.

Исследуется магнитное поле импульсных соленоидов. Произведена оценка аксиального поля, используя аналитический и численный методы. Полученные результаты сравниваются с данными эксперимента по измерению аксиального поля с помощью индуктивного датчика и датчика на основе *LaCaMnO* материала. Отмечается хорошее соответствие экспериментальных и вычисленных результатов. Ил. 12, библи. 10 (на английском языке; рефераты на английском, литовском и русском яз.).

